

‘Charybdis’ – The Next Generation in Ocean Colour and Biogeochemical Remote Sensing

Christopher Lowe & Malcolm Macdonald
 Advanced Space Concepts Laboratory, University of Strathclyde
 Mechanical and Aerospace Engineering, 347 Cathedral Street, Glasgow, G1 2TB, UK
 +44 (0)7841 666329
 christopher.lowe@strath.ac.uk

Steve Greenland
 Clyde Space Ltd
 Clyde Space Ltd, Helix Building, Kelvin Campus, West of Scotland Science Park, Glasgow, G20 0SP, UK
 +44 (0)141 946 4440
 steve.greenland@clyde-space.com

David Mckee
 Marine Optics and Remote Sensing Group, Dept. of Physics, University of Strathclyde,
 John Anderson Building, 107 Rottenrow, Glasgow, G4 0NG, UK;
 +44 (0)141 548 3068
 david.mckee@strath.ac.uk

ABSTRACT

Within the field of Space-based Maritime observation, there exists an opportunity in the form of high spatial, high temporal resolution multi-spectral imaging to map coastal and inland waterway colour and biogeochemistry. Information provided would help environmental agencies and the scientific community to better understand patterns and evolution of ecological systems, sediment suspension in river estuaries and the effects of anthropogenic processes on our water systems. In addition, monitoring of these colour patterns with respect to the well understood tidal sequence would provide significant benefits to our understanding of the way in which tidal forcing affects ocean colour.

This paper describes the astrodynamics properties of a tidal-synchronous satellite trajectory and the system-level design of a multi-platform CubeSat constellation capable of high resolution, multispectral imaging. The constellation, named ‘Charybdis’, is envisaged to be dedicated to providing unprecedented levels of data (high temporal and spatial resolution) of coastal regions and inland waterway colour and biogeochemistry. Analyses of two alternative missions are presented; one providing bi-hourly, global coverage from 115 nanosatellites and a second providing bi-hourly regional coverage over the UK mainland from 30 nanosatellites.

INTRODUCTION***Ocean Colour***

The colour of the ocean is defined by the visible radiance reflected from the upper layers of the water, which varies widely throughout the world from bright turquoise clear oceanic waters, through green algal blooms to deep brown, murky waters of a recently dredged commercial port. Being able to analyse ocean colour is a vital tool which enables users to better understand a multitude of processes.

By far the dominant use of ocean colour data is for the purpose of phytoplankton concentration assessment. Understanding where these species are located and how they evolve over time can improve our understanding of climate change, aid the development and operation of

fisheries and help us to monitor wildlife behaviour and decline.

Another major use of ocean colour is to better understand biogeochemical cycles which are presented in the form of vast pools of carbon at the surface of the Earth. These Carbon reservoirs exist in many forms, including Particulate Organic and Inorganic Carbon (which encompasses plankton, bacteria, detritus, faecal pellets and Calcium Carbonate), Phytoplankton Carbon and Dissolved Organic Matter (DOM, the coloured fraction often being referred to as ‘yellow substance’). Measurement of the time dependent biogeochemical cycles, made visible through carbon pool location and concentration data, provides important input to computational climate change models.

Furthermore, information specific to coastal waters, such as mixing of fresh water and salt water, water

quality, hazardous events (oil/sewage spills and harmful algal blooms) port operations and violation of international shipping & environmental regulations, can be obtained in the form of ocean colour data.

It is for these reasons, and many more, that remote sensing of the oceans continues to be a major component of many Space Agency environmental mission portfolios.

Tidal Theory

Variation in sea surface height (commonly known as tide) is a phenomenon present in the majority of oceanic regions and has significant impact on commercial, ecological and biological systems worldwide. Most places on Earth experience a regular periodic variation in sea-level of approximately two high tides and two low tides per day (semi-diurnal tide), while other regions exhibit diurnal tides or a combination of the two. Regardless of pattern, all tides are driven by gravitational influence on the oceans by the Moon and Sun, as the Earth rotates about its axis, the Moon rotates about the Earth, and the Earth-Moon system rotates about the Sun.

Variation in the tidal range is also affected by gravitational forces from external bodies, with the primary driver being the difference in position of the Sun and Moon, with respect to the Earth. Approximately at the time of alignment between the Sun, Moon and Earth, the greatest tidal range (Spring tide) is experienced while the lowest range (Neap tide) occurs shortly after a separation of 90° between the three celestial bodies (Figure 1).

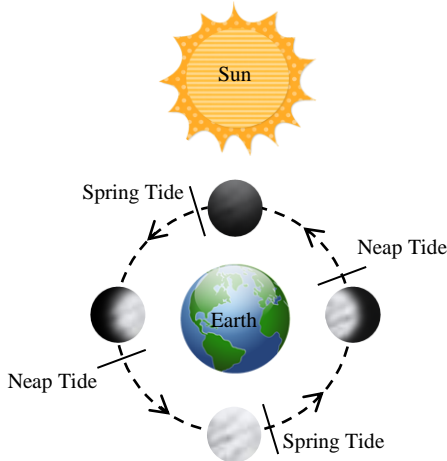


Figure 1: Variation in tide-type with respect to Sun and Moon position

Other factors exist which play a significant part in range, and a minor part in periodic regularity, such as orbit eccentricity of the Moon around the Earth, orbit eccentricity of the Earth around the Sun, obliquity of the Earth Equator to the ecliptic, bathymetry, barometric pressure and wind speed. It is the

combination of all these effects that results in no two locations on Earth having identical tidal properties. Tidal range can vary from a few centimetres in the Mediterranean Sea, to up to 16.3m in the Bay of Fundy, Canada and as such, the tide can play a key role in many natural and anthropogenic processes.

Tidal Effects on Ocean Colour

One of the major limitations of current ocean colour observations is the once-per-day temporal resolution capability. The ability to monitor short term effects caused by tidal variation would add a new dimension to the information gathered and, in particular, being able to model ocean colour variation as a function of tidal condition would be a significant advancement.

Tide-induced currents can result in significant errors between sets of data obtained at differing tidal states, such that comparison becomes almost impossible without sophisticated validation methods, which do not exist at present.¹ An alternative approach, presented here for the first time, is to capture data at regular, known tidal states, such that comparison between equivalent data can be performed without relative error.

Image Resolution and Ocean Colour

The benefits associated with increased spatial resolution of ocean colour data become increasingly clear as analysis approaches the coastline and inland, trending towards ports, rivers and sea-lochs/fjords. Data available currently in these regions is either of insufficient detail, or insufficient frequency (aircraft imaging and in-situ measurements), such that higher resolution sensors would enable new information to be obtained. In addition, monitoring of specific events out at sea such as oil-spills could be conducted with significantly greater accuracy with greater spatial resolution.

An increase in temporal resolution also has many benefits, such as;

- i. Additional data available with which patterns in ocean colour over the long term can be assessed.
- ii. Additional data available relating to the effects of tidal streams on ocean colour over the tidal period.
- iii. Improved coverage to exploit gaps in cloud cover.

OCEAN COLOUR FROM SPACE

Single Platform Mission

Space-based remote sensing of ocean colour has been delivered from Earth Observation platforms since the launch of NASA’s Nimbus-7 satellite in 1978, which carried the ‘Coastal Zone Color Scanner’ (CZCS).

Since CZCS, 23 instruments have been deployed to provide ocean colour measurements, twelve of which have now been decommissioned.

The majority of ocean colour sensors, including SEAWiFS, MODIS & MERIS, have operated from Sun-Synchronous (SS) LEO, and provide multi-spectral imaging with spatial resolution in the order of hundreds of metres and temporal resolution of the order of one day.² Exceptions to this include the South Korean built 'GOCI' instrument which occupies a Geostationary position and provides continuous medium resolution images of the Far-Eastern regions, and the US-DoD built 'HICO' which orbits on-board the International Space Station (ISS).

Data from the 'Compact High Resolution Imaging Spectrometer' (CHRIS), on-board the PROBA satellite, have been applied to ocean colour analysis to good effect.^{3,4} Images with 36m resolution over 62-bands are evaluated and it is seen that evaluation of suspended particulate matter in particular show promise. Due to the relatively small size of PROBA (94kg), compared to other ocean colour satellites, a constellation of these platforms for future coverage has huge potential.

The first sensor (specific for ocean colour imagery) designed to exceed the historic typical spatial resolution is the DLR-built 'HSI' instrument, on-board EnMAP, which is due for launch in 2015 and has a Ground Spectral Density (GSD) of 30m.⁵ This resolution would provide a leap forward in terms of information available to users; however the ever-present trade-off between temporal and spatial resolution is clear, with repeat visits available only every four days.⁵

Multi-Platform Missions

There are currently no stand-alone constellations scheduled with ocean colour imaging capability, however the IOCCG are investigating the use of a 'virtual' constellation in order to exploit data from numerous sources (both satellites and in-situ devices) which complement each other toward a complete dataset for ocean colour radiance. The ocean Colour Radiometry Virtual Constellation (OCR-VC) has been approved by the Committee on Earth Observation Satellites (CEOS) and outlines some of the basic requirements of future ocean colour sensors [OCR-VC white paper].

CubeSat Imaging

A study into the use of a 3U CubeSat to conduct high resolution (30m), multi-spectral imaging specific to ocean colour has been conducted previously.⁶ The payload supports a 3-colour (RGB) linear array plus an additional luminance linear array, and is shown to be capable of high quality imaging on a small, low-cost platform. Some degree of development in the spectral

properties is considered necessary to rival current dedicated ocean colour sensors; however the potential for increased temporal resolution and system robustness is great.

The Miniature Imaging SpaceCraft (MISC) is another example of a nanosatellite capable of multi-spectral imaging, potentially applicable to ocean colour analysis. Again, a 3U CubeSat platform is employed, which is capable of multispectral imagery at 7.5m spatial resolution, from an altitude of 540km.⁷

TIDAL SYNCHRONISM

Theoretical Definition

It is common for Earth imaging satellites to be deployed into a 'Sun-Synchronous' (SS) orbit, whereby the Earth-Sun vector remains constant with respect to the satellite orbit plane throughout the mission lifetime. This allows visible images of particular ground locations to be captured regularly, with consistent illumination conditions, over long periods of time. Since the driving force behind a great deal of marine systems is the tide, and the majority of oceanic locations on Earth are influenced significantly by the Lunar Semi-diurnal Constituent (M_2), an orbit trajectory synchronous with this tidal forcing function is considered as a potential alternative. For the first time, a 'Tidal-synchronous' (TS) orbit is described, and applied to a novel ocean colour imaging satellite constellation.

Since the Moon orbits the Earth in the same direction that the Earth rotates about its polar axis, the duration between consecutive passes of the Moon through a particular hour angle is slightly greater than a Sidereal Day. It takes approximately 24.84 hours for a complete revolution of the Earth with respect to the Earth-Moon vector (Sidereal Day is 23.934 hours) and is termed a 'Tidal Lunar day' (TLD = τ_r seconds) (Figure 2, dot represents point of interest on Earth surface at High tide condition).

Where θ = angle of rotation of a particular point on Earth with respect to the vernal equinox after one TLD. A TS orbit can therefore be defined as an orbit in which a future Sub-Satellite Point (SSP) coincides with a particular location on Earth at the same time in its tidal sequence (i.e. after an integer number of TLDs).

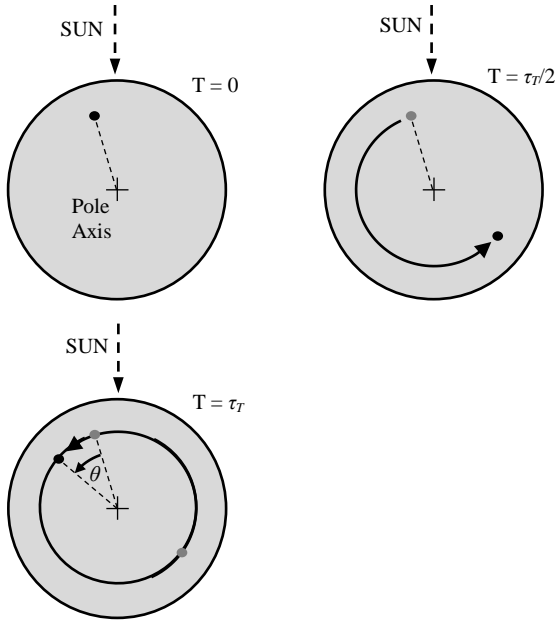


Figure 2: Angular rotation of Earth after one TLD

Astrodynamic Requirements

In order to satisfy the requirement of tidal synchronism detailed above, the orbit plane in which the satellite exists must be subject to a steady rotation in Right Ascension of Ascending Node (RAAN). A certain magnitude of RAAN rotation can be achieved through exploitation of natural perturbations in the Earth gravity potential, which is possible due to the Earth's non-spherical nature. The magnitude and direction of the rotation achieved depends on the number of TLDs before repeat SSP (m), and the number of satellite orbits before repeat SSP (n), both of which must be specified by the user. In order to define the orbit characteristics necessary to satisfy the above parameters, the amount of rotation (θ_1 , radians) that the Earth experiences during the specified number (m) of TLDs must be analysed:

$$\theta_1 = 2\pi \frac{m\tau_T}{\tau_E} \quad (1)$$

Where; τ_E = duration of a Sidereal Day (seconds).

Subtracting this amount of rotation, θ_1 , from the rotation experienced by the Earth over the nearest number of complete Sidereal days (θ_2 , radians), the amount of rotation in RAAN required (ϕ) over the repeat period can be calculated:

$$\phi = \theta_2 - \theta_1$$

Where;

$$\theta_2 = 2\pi\zeta \quad (2)$$

$$\zeta = \left\lceil \frac{m\tau_T}{\tau_E} + 0.5 \right\rceil \quad (3)$$

Where; ζ = nearest integer number of Sidereal days between SSP repeats, such that;

$$\phi = 2\pi \left(\zeta - \frac{m\tau_T}{\tau_E} \right) \quad (4)$$

The amount of rotation in RAAN required per orbit ($\Delta\phi$) can therefore be calculated, based on the satellite orbit period (τ);

$$\Delta\phi = \frac{2\pi\tau}{\tau_r} \left(\frac{\zeta}{m} - \frac{\tau_T}{\tau_E} \right) \quad (5)$$

Where;

$$\tau = \frac{m\tau_T}{n} \quad (6)$$

Using analytical approximations (considering only the J_2 oblateness term and only variation in RAAN with time), semi-major axis (a) and inclination (i) can be defined;⁸

$$a = \left[\mu \left(\frac{\tau}{2\pi} \right)^2 \right]^{1/3} \quad (7)$$

Where, μ = Earth gravitational constant ($3.986 \times 10^{14} \text{ m}^3\text{s}^{-2}$).

$$i = \cos^{-1} \left[\frac{-\Delta\phi a^2 (1-e^2)^2}{3\pi J_2 R_E^2} \right] \quad (8)$$

Where, e = orbit eccentricity (defined as zero in the case of Charybdis), R_E = Earth mean volumetric radius (6371 km) and J_2 = Earth oblateness coefficient ($1.083e^{-3}$).

The TS orbit parameters can be defined further by restricting the repeat SSP frequency to an exact number of Earth rotations (p), with respect to position of the orbit plane, and corresponding number of satellite orbits (q), such that:

$$n = \frac{\zeta q}{p} \quad (9)$$

Where the following must be met in order to maintain tidal synchronism:

$$\frac{n}{q} = \frac{\zeta}{p} \in \mathbb{Z}$$

This additional requirement, whilst limiting the choice of orbit altitude and inclination combinations, has benefits for missions in which only a specific region of interest exists. For example, setting $p = 1$ results in the satellite passing overhead a particular location each day, such that complete daily coverage of a specific area can be achieved using fewer satellites than with an arbitrary selection of m & n .

Positioning of the satellite within its orbit, via definition of the Argument of Perigee (ω), RAAN (Ω) and True Anomaly (ν), is not considered necessary at this stage of the mission design.

MISSION REQUIREMENTS

Orbit Requirements

Almost all Space missions have requirements with respect to orbital characteristics, and for Earth observation platforms these generally include;

- i. Minimum acceptable observed latitude range, which is a function of inclination
- ii. Acceptable orbit altitude range, for given payload spatial resolution and lifetime (drag effects).

As such, orbital requirements for ‘Charybdis’ platforms are outlined (Table 1):

Table 1: Charybdis Orbit Requirements

Parameter	Value	Comment
Altitude (r)	500 – 800 km	Necessary for imager resolution and launch cost.
Inclination (i) – Global coverage	> 80°	Necessary to ensure visibility of high latitudes.
Inclination (i) – Regional coverage	Function of Latitude	Dependent on region of interest.
Eccentricity (e)	0	Necessary to ensure image consistency worldwide.
RAAN rotation rate ($\Delta\phi$)	~360°/year [†]	As close to SS orbit conditions as possible

[†] In the case of visible imaging payloads, the additional requirement of Sun synchronism often exists such that illumination conditions remain constant over the entire mission lifetime. As with TS orbits, naturally perturbed SS orbits also function only with certain combinations of semi-major axis and inclination parameters, however identical combinations for both TS and SS orbits do not exist for repeat parameters considered reasonable by the author. Should steady illumination conditions be considered a requirement, the repeat parameter, m , can be selected such that a rotation in RAAN is as close as possible to that required for Sun synchronism (where $\Delta\phi = 360^\circ/\text{year}$).

Constellation Requirements

In order to provide both high spatial resolution and high temporal resolution, ‘Charybdis’ must be deployed as a constellation of satellites. To minimise cost and development time, the CubeSat platform is baselined and each satellite in the constellation shall be of identical design.

The minimum number of orbit planes required to achieve bi-hourly temporal resolution (coverage every other hour) during daylight hours (0800hrs – 1600hrs) shall exist, in order to minimise launch cost. This equates to five equi-spaced orbit planes, and hence a potential minimum of five launches.

Payload Requirements

Considering current system capabilities, future prospects in ocean colour observation and demand from the scientific community, the following payload performance metrics are considered necessary for mission success (Table 2):

Table 2: Payload Requirements

Parameter	Value	Comment
Spatial Resolution (R_s)	30m, or better	Necessary to match current and future capabilities and provide useful data for inland waterways.
No. of Wavebands	7	Minimum considered necessary to provide useful ocean colour data.
Bit per sample	10 bit	Equivalent to SeaWiFS instrument capability

System performance on this scale, in combination with bi-hourly coverage, will provide dramatic improvement in the data available to scientists across the globe and could revolutionise ocean colour analysis. In particular, the increase in spatial resolution will enable analysis of inland waterways and complex coastal regions, which have previously been inaccessible from ocean colour sensors.

The ‘International Ocean Colour Coordinating Group’ (IOCCG) has outlined properties of ocean colour sensors considered necessary to measure ocean colour with an acceptable level of accuracy.⁹ The number of, and width of, frequency bands captured by the detector must be defined by the user, dependent on information to be analysed. As such, the payload capability considered necessary by the authors is summarised, along with associated frequency parameters (Table 3). This includes capability to analyse Phytoplankton (Chlorophyll), Suspended Sediment, Coloured Dissolved Organic Matter (CDOM) and correction of atmospheric effects.

Table 3: Payload Spectra of Interest

Area of Interest	Central Wavelength (nm)	Bandwidth (nm)
CDOM	412	10
Phytoplankton (Chlorophyll)	440	10
	490	10
	555	10
Suspended Sediment	667	10
Atmospheric Correction	750	14
	870	20

Multi-spectral, high resolution imaging capability has already been demonstrated on board CubeSat platforms such that high levels of confidence exist in these requirements being met.⁷

Spatial Resolution Limit

Considering the above spectra of interest (Table 3), payload focal length (f) and payload aperture diameter (D), the limit of spatial resolution (on the detector plane) (Δl_{Ray}) can be calculated from the Rayleigh Criterion:

$$\Delta l_{Ray} = 1.22 \frac{f \lambda}{D} \quad (10)$$

As long as this resolution limit is smaller than the pixel size of the detector, the resolution will be limited by the payload and orbit parameters, and not be 'diffraction limited'. Assuming a payload aperture of 75mm, wavelength of 890nm and a focal length of 100mm, a Rayleigh limit resolution exists of the order:⁶

$$\Delta l_{Ray} = 1.45 \mu m$$

The actual detector resolution limit (Δl_{Ray}) shall be calculated for the specific constellation properties, since the payload focal length and aperture diameter can be optimised in order to achieve the prescribed spatial resolution and F-number, at any given orbit altitude. This will provide a suitable payload design at minimum mass.

In a similar manner, the Ground Separation Distance limit (GSD_{lim}), which represents the distance between two objects distinguishable on the Earth surface, can be calculated:

$$GSD_{lim} = 1.22 \frac{r \lambda}{D} \quad (11)$$

Where r = orbit altitude. As long as the theoretical maximum spatial resolution achievable by the payload is greater than this value (30m in the case of 'Charybdis'), the image should not be limited by this phenomena.

MISSION DESIGN

Astrodynamic Properties

The astrodynamic requirements (Table 1) result in additional restrictions to the repeat parameters available, since only a certain range of $\Delta\phi$ can be achieved over this range. It emerges that the minimum value of m (Tidal Lunar Days before repeat GT) suitable is 25 for global coverage and as little as 18 for regional coverage (up to 25° Latitude). It should be noted that a greater value of m results in a greater period of time before similar tidal conditions are observed, at a particular location, by a particular platform. However, bi-hourly coverage of any ground location is possible in all instances.

Since the 'Charybdis' mission will aim to monitor ocean Colour, sensing in the visible spectrum is required. This characteristic lends itself to consistent illumination conditions, which has already been established as impossible to the extent available for SS orbits. It is however possible to achieve something relatively close to SS conditions, with $m = 57$ TLDs, resulting in a rotation in RAAN of 355.22°/year (i.e. shift in Sun illumination angle of <5°/year). It is therefore considered that 57 TLDs before repeat SSP shall be the baseline for the Charybdis mission.

The value of n can now be specified in order to define altitude and inclination parameters, either in isolation (suitable for global coverage) or with the additional limitations recommended for regional coverage (p & q , from Equation 9). Two possible orbits are defined (Table 4), on which system-level design shall be described. The first, Mission A, provides global coverage with an altitude comparable to previous ocean colour missions such as SeaStar (SeaWiFS) and Aqua (MODIS), both of which fly at an altitude of ~705km. Mission B is suitable for regional coverage such that daily repeat ground tracks are achieved with each platform ($p = 1$).

Table 4: Orbit Parameters for two Missions

No.	M	n	p	q	Altitude (r) (km)	Inclination (i) (Degrees)
A	57	860	-	-	707.8	98.1
B	57	885	1	15	573.9	97.6

Constellation Properties (Global Coverage)

In order to obtain bi-hourly repeat visits from the constellation, it is necessary for a series of orbit planes to exist with separation in RAAN equal to 30° between them. Assuming worldwide 'daylight' hours exist between 0800hrs and 1600hrs, then with one orbit plane per two hours, five planes ($N_{Plane} = 5$) would be required. The total number of platforms (N_{Plat}) will

therefore equate to the number of Spacecraft per plane ($N_{S/C}$) multiplied by the total number of planes (N_{Plane}).

In order to achieve continuous coverage from ‘Charybdis’, a train of spacecraft is proposed for each plane such that as the Earth rotates underneath the plane, coverage of all ground locations is made. This ensures minimum number of orbit planes for complete coverage, which generally results in minimum launch cost.

Constellation Properties (Global Coverage)

The quantity of spacecraft required in each plane can be written as a function of the orbit and payload parameters (at the equator). Note that complete coverage at the equator will ensure at least complete coverage at all other Latitudes. The number of spacecraft per orbit plane ($N_{S/C}$) can be written as:

$$N_{S/C} = \frac{2\pi}{\Delta v} \quad (12)$$

Where; Δv = true anomaly separation between S/C in the orbit plane. By evaluating two consecutive platforms crossing the equator, a point on the ground at the edge of the image captured by the first platform (S/C₁) must be captured at the opposite edge of the image of the second platform (S/C₂) in the train (Figure 3).

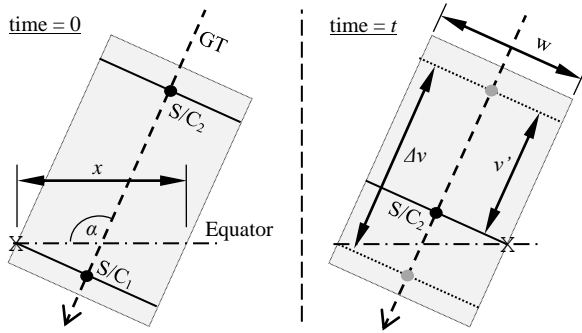


Figure 3: Equator Crossing Coverage

Where; GT = ground track of the satellites, w = Swath Width (m), α = ground track angle (equal to inclination at equator) (radians), x = angular distance travelled by point X on Earth surface and v' = true anomaly angle travelled by each platform in time t .

From geometry, assuming that Swath Width is measured on a ‘flat’ Earth, angle x can be written as:

$$x = \frac{w}{R \sin \alpha} = \frac{2\pi t}{\tau_E} \quad (13)$$

Where; $R = R_E$ = Earth equatorial radius (6378km) and τ_E = Sidereal day (86164 seconds). The angular distance

travelled by the spacecraft (v'), over time t , can also be specified:

$$v' = \frac{2\pi t}{\tau}$$

Where; τ = satellite orbit period (seconds). Substituting τ from Equation 6, v' becomes:

$$v' = \frac{2\pi t n}{m \tau_T} \quad (14)$$

Rearranging Equation 14 and substituting for t :

$$v' = \frac{n x \tau_E}{m \tau_T} = \frac{n w \tau_E}{m R \tau_T \sin \alpha} \quad (15)$$

Also from geometry, the maximum theoretical value for Δv (Δv_{Max}) can be written as:

$$\Delta v_{Max} = v' - x \cos \alpha \quad (16)$$

The theoretical minimum number of spacecraft per plane ($N_{S/C}$) can therefore be calculated by substituting Δv_{Max} into Equation 12 and rounding up to the nearest integer:

$$N_{S/C} = \left\lceil \frac{2\pi}{\Delta v_{Max}} \right\rceil \quad (17)$$

The actual value of Δv can then be calculated from rearrangement of Equation 12. It is clear that for a fixed value of swath width (w), i.e. fixed values of spatial resolution and cross-track pixel number, and a fixed value of m (57), the number of S/C per orbit plane decreases with increasing values of n . As a result, the number of S/C per plane can be plotted against altitude (Figure 4):

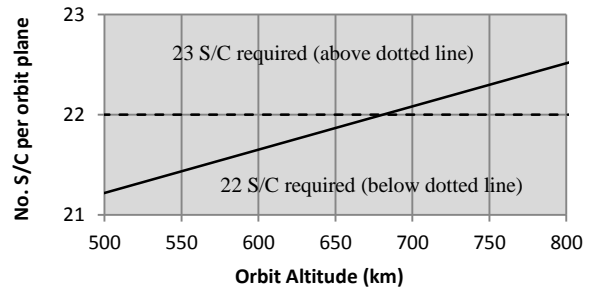


Figure 4: Plot of $N_{S/C}$ vs. Orbit Alt (km)

The total number of platforms (N_{Plat}) required in the constellation can now be calculated, based on a temporal resolution of bi-hourly repeats between ~0800hrs and ~1600hrs (5 planes) for the two missions (A & B) (Table 5):

Table 5: Total number of platforms (N_{Plat})

Mission	Alt. (km)	Platforms per Plane ($N_{S/C}$)	Total platforms for Global coverage (N_{Plat})
A	707.8	23	115
B	573.9	22	110

Constellation Properties (Regional Coverage)

As mentioned previously, monitoring of certain regions only is likely to require fewer S/C than is required for global coverage, for similar values of m & n (with the additional limitations of p & q). A general solution to the true anomaly separation between S/C in the orbit plane can be found through use of more general terms for the ground track angle, α , and radius parameter, R . Whilst the assumptions; $\alpha = i$ and $R = R_E$ were acceptable for evaluation of coverage at the equator, variation in latitude must be accounted for in the general case and as such, changes to the above equations must be made:^{10 11 12}

$$R \rightarrow R_{Lat}$$

Where,

$$R_{Lat} = R_{Geo} \cos L = \cos L \sqrt{1 + \sin L \left[\frac{R_E^2}{(1-f)^2} - 1 \right]}$$

And,

$$\alpha = \frac{\pi}{2} - \arcsin\left(\frac{\cos i}{\cos L}\right)$$

L = minimum latitude of region of interest (radians), f = Earth Flattening parameter (1/298.26), R_{Geo} = Geocentric Radius (m) and R_{Lat} = Radius from latitude of interest to polar axis (m) (Figure 5):

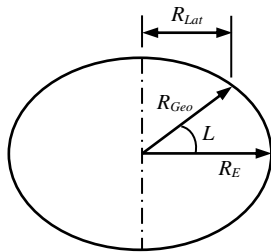


Figure 5: Latitude Radius

Substituting the above values of R and α into Equation 13, 15 and 16, the solution to Δv_{Max} in terms of inclination (i) and minimum latitude (L) of the region of interest can be found. The number of S/C required (per plane), to achieve complete coverage at that specific latitude can then be found via Equation 17, which is

acceptable up to latitudes approaching the following condition:

$$L \geq \pi - \lambda - |\pi - i|$$

Where, λ = Swath half-angle (radians);

$$\lambda = \frac{w}{2R_{Geo}}$$

At which point the ground track angle (α) tends to zero and x tends to infinity. The number of S/C required to provide complete coverage (at a particular latitude) is plotted against latitude, for Mission B (altitude 573.9km) (Figure 6):

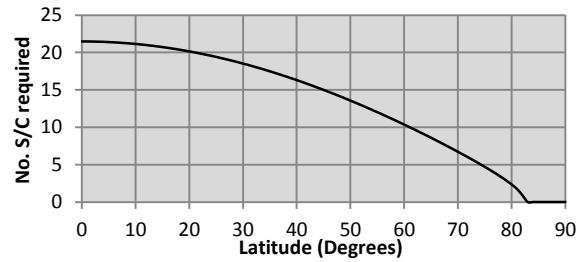


Figure 6: No. S/C required for complete Latitude coverage vs. Latitude

Furthermore, for a region with limited Longitude range, $\Delta\delta$ (e.g. the UK mainland which is bound by approximately 2°E and 8°W and has a minimum Latitude boundary at ~50°N), the number of S/C required for complete coverage of that region can be calculated. In other words, the orbit plane need not be fully populated:

$$\Delta\delta = +2^\circ - -8^\circ = 10^\circ$$

$$L \sim 50^\circ$$

$$N_{S/C} = \left\lceil \frac{\Delta\delta}{x} \right\rceil = 6 / \text{Plane} \tag{18}$$

So for complete, bi-hourly coverage of the UK mainland during daylight hours (0800hrs – 1600hrs), Charybdis would require 6 S/C per plane, and 30 S/C in total.

It might be considered desirable to position the satellites in such a manner as to enable extension of the system to global coverage at minimum cost. In order to achieve this, True Anomaly spacing equivalent to that required for global coverage would be employed, with the number of platforms chosen such that only the region of current interest is covered. Again, for the UK mainland, this constitutes 10 platforms per plane, at a TA separation of ~15.6°, whereby addition of 12 more

platforms per plane would enable complete coverage (Table 5).

Mission Lifetime

Continuous provision of ocean colour data in the long term is a critical factor in the development of a new mission within this field. As such, the total cost of design, development, deployment, operation and replenishment of the system becomes the parameter of interest. For example, a system designed in 1 year, to operate for five years, costing €10m (cradle to grave) would be more cost effective than an alternative platform designed in 5 years, to operate for 15 years, costing €100m. This philosophy is becoming increasingly important with the growth in popularity of small, low cost satellite systems.

Nonetheless, lifetime of an individual platform remains a critical factor and continues to drive the system design. Subsystems must operate to a certain standard at the end of life (EoL) and sufficient propellant may be required to maintain orbit parameters to within acceptable limits, despite perturbations from atmospheric drag, solar radiation pressure and magnetic disturbances. Since a tidal-synchronous orbit requires precise station-keeping (constant m & n parameters), some form of on-board propulsion is considered critical for altitudes <800km. Early system-level design of the propulsion system can be achieved based on perturbations due to atmospheric drag effects in isolation. The Force F_D (N) exerted on a body of mass M (kg), with projected surface area S (m²), drag coefficient C_D , travelling at velocity V (m/s), through a gas with density ρ (kg/m³), is defined as:

$$F_D = \frac{1}{2} \rho V^2 S C_D \quad (19)$$

Where the atmospheric density (based on the 1976 US standard atmosphere model¹³) can be approximated as a function of orbit altitude r (km), through application of a power law:¹⁴

$$\rho = \Lambda r^{-\gamma} \quad (20)$$

Where; $\Lambda = 10^7$ and $\gamma = 7.201$. From these relationships, the total propellant mass M_p (kg) required to compensate for atmospheric drag over a mission of lifetime, L (seconds), can be calculated, given a certain Specific Impulse capability I_{sp} (seconds):

$$M_p = \frac{L F_D}{I_{sp} g} \quad (21)$$

The ΔV required from the system to overcome atmospheric drag (ΔV_D) can subsequently be calculated:¹⁰

$$\Delta V_D = I_{sp} g \ln \left(\frac{M}{M - M_p} \right) \quad (22)$$

A number of micro-propulsion systems currently exist, or are under development, which are suitable for CubeSats and provide promising levels of performance to satisfy the requirements outlined above.^{15 16 17} A plot of propellant mass per year, versus altitude, for a 3U CubeSat (long face normal to velocity vector) at altitudes between 500km – 800km, with mass of 5kg and drag coefficient of 2.1, is shown for propulsion systems with I_{sp} of 100s, 500s and 1000s (Figure 7):

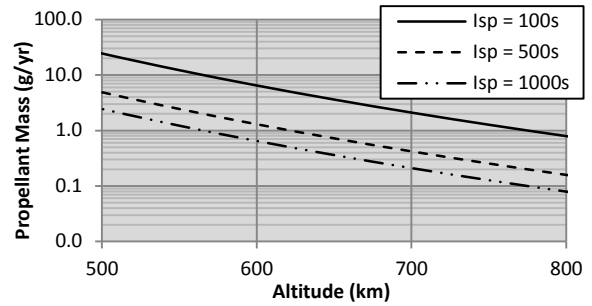


Figure 7: Plot of Propellant Mass (g/yr) required to compensate for Drag, vs. Orbit Altitude (km)

Post Operation De-Orbit

In order to satisfy orbit debris mitigation requirements outlined in¹⁸, post operational orbit lifetime must be no longer than 25 years.¹⁸ De-orbiting to an altitude sufficiently low to ensure imminent destruction through atmospheric heating (assumed to occur at 100km) could be achieved via a combination of the naturally occurring atmospheric drag and use of on-board propulsion. It is considered that other mechanisms of orbit decay (e.g. drag sails and electro-dynamic tethers) would be mass and volume inefficient, given that a propulsion system is necessary for station-keeping.

Below a certain critical altitude (r_{crit}), atmospheric drag will provide all the necessary force for re-entry to occur within 25 years. As such, all times prior to reaching this critical altitude shall be considered ‘operational’ and hence will not contribute to the 25 year decay requirement. Evaluating the problem from the principal of energy conservation, the rate of change of two-body specific energy can be defined by:

$$\dot{E} \cong -\frac{1}{M} FV \quad (23)$$

Where velocity (V), assuming quasi-circular orbit, is:

$$V_{circular} = \sqrt{\frac{\mu}{R}} \quad (24)$$

And, specific energy (E) is:

$$E = \frac{-\mu}{2R} \quad (25)$$

Substituting for F , ρ and V from Equations 19, 20 and 24 respectively, and integrating between initial (R_0) and re-entry (R_F) orbit radii, the natural de-orbit (drag-only) lifetime (L_{DD}) can be derived:¹⁴

$$L_{DD} = \frac{1000^{-\gamma} M}{C_D \Lambda A \sqrt{\mu R_E}} \frac{((R_0 - R_E)^{1+\gamma} - (R_F - R_E)^{1+\gamma})}{1 + \gamma} \quad (26)$$

At the operational radius (R_0) where this natural de-orbit lifetime (L_{DD}) equals 25 years, operations could be halted and drag-induced decay and burn-up would be allowed to occur. This critical radius (r_{Crit}), is identified as ~6952km (altitude of ~581km, Figure 8), for the configuration described here (3U, 5kg).

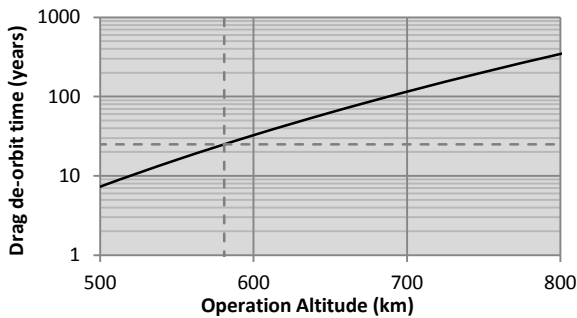


Figure 8: Drag De-orbit time (years) vs. Operational Orbit Altitude (km)

The time required to decay from operational altitude to this critical altitude depends of course on the operational altitude itself, and the propulsion system properties. The least costly solution in terms of propellant would be to simply allow drag to decay the orbit, regardless of the operational altitude, however this is costly in terms of time (increasingly so with altitude), which of course results in greater operational cost. At this stage therefore, it is assumed that a thrust of $1\mu\text{N}$ can be provided by the propulsion system and a plot of propellant mass & time to reach critical altitude vs. operational altitude is shown (Figure 9).

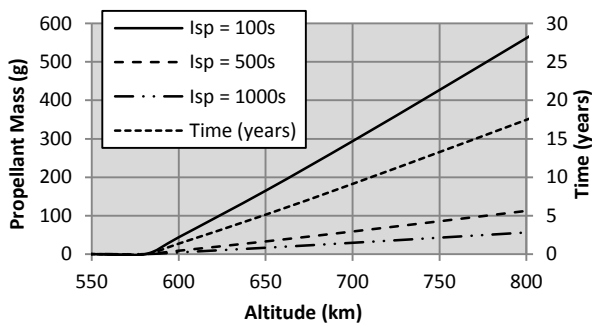


Figure 9: Fuel required & time to decay to Critical Altitude vs. Operational Altitude

For the two missions (A & B) considered (altitudes of 707.8km and 573.9km), the amount of propellant (for $I_{SP} = 500\text{s}$) and time required to lower the orbit to the critical de-orbit altitude (~581km) is shown (Table 6):

Table 6: Orbit lowering performance ($I_{SP} = 500\text{s}$)

Mission	Altitude (km)	Propellant required (g)	Time to reach r_{Crit} (years)
A	707.8	62.8	9.77
B	573.9	0	0

PLATFORM DESIGN

Structure and Configuration

Each platform in the ‘Charybdis’ constellation shall be identically designed and follow the CubeSat standard.¹⁹ A baseline size (U -scale) of the platform shall be 3U (maximum for use of standard P-POD deployment system), however the size is dependent on the volumetric subsystem requirements based on the specific orbit parameters into which the system is deployed. As such, it is proposed that optimisation of the platform size is carried out in the future.

The structure shall be made from Aluminium 7075 or 6061, unless thermal analysis dictates otherwise, to ensure sufficient specific stiffness and specific strength properties.¹⁹ The effects of thermal expansion on the quality of optical data must be quantified during future work.

Electrical Power System

The Electrical Power System (EPS) provides the power necessary to maintain spacecraft functionality over the mission lifetime, converting solar energy during sunlit conditions (via ‘Spectrolab’ Ultra Triple Junction solar arrays) and stored chemical energy during eclipse (via ‘Clyde Space Ltd’ Lithium Polymer batteries). An active ‘maximum power point tracking’ (MPPT) philosophy shall be employed, such that excessive power is not required to be dumped as heat during the mission.

The solar array area (panel configuration) and battery capacity required is dependent on the constellation parameters such that it will be mass optimised in order to satisfy power demand without excessive over-design. The baseline solar array configuration will comprise body-mounted panels, with deployable arrays added if necessary.

Propulsion System

As discussed previously, requirements for the propulsion system are dependent on the selection of orbit altitude at which Charybdis shall operate. Drag compensation during the operation phase and de-orbit

assistance drive the design in terms of performance, while configuration and volume drive the geometric properties.

To minimise attitude control requirements, the thrust vector from the propulsion system will act directly through the S/C centre of mass, while drag compensation dictates a thrust vector tangential to the orbit (for a circular orbit). Assuming a uniform distribution of mass, the propulsion system should be positioned at the mid-point of the structure, with the thrust vector aligned normal to the Nadir and angular momentum directions. The primary impact of this is limitation on the volume available for payload, in particular limitation on the focal length. To a certain extent, this limitation can be mitigated through application of a catadioptric lens arrangement, although additional aperture diameter and complexity would be required.

Payload

The payload on-board each Charybdis platform shall consist of a narrow angle camera capable of multi-spectral imaging across seven wavebands spanning 407nm to 880nm (Table 3). Fixed properties of the payload CCD detector are described (Table 7):

Table 7: CCD Detector Properties

Payload Property	Value	Comment
Array Size	7 x 4080 active pixels	Linear array for each Waveband
Pixel Size (Δl)	5 μm (square)	Commercially available
F-number (focal length/aperture ϕ)	2.5	Minimise chromatic aberration for size
Bits per sample	10 bit/sample	Consistent with SeaWiFS imager
Ground spatial resolution	30 m	Suitable for inland waterways
Data/Area	0.077 bit/m ²	Function of payload properties

Since this study aims to compare various constellation parameters against pre-defined payload performance (resolution), the payload focal length (f) is optimised as a function of orbit altitude (r), for constant pixel size ($\Delta l = 5\mu\text{m}$) and spatial resolution ($R_S = 30\text{m}$):

$$f = \frac{\Delta l \cdot r}{R_S} \quad (27)$$

Lens aperture diameter (D) can now be defined as a function of focal length and F-number (F):

$$D = \frac{f}{F} \quad (28)$$

The focal length and aperture diameter for each mission is detailed below (Table 8):

Table 8: Focal Length (for spatial resolution of 30m)

Mission	Altitude (km)	Focal Length (mm)	Aperture Diameter (mm)
A	707.8	118	47
B	573.9	96	38

Both of the specified focal lengths allow for accommodation of the payload within the initial half of CubeSat such that the propulsion system is able to provide thrust through the S/C Centre of Mass. Furthermore, the above defined properties result in satisfactory Rayleigh limits, based on Equation 10.

Attitude Determination and Control System

In order to achieve and maintain acceptable pointing accuracy of $<1^\circ$, a 3-axis stabilised system comprising miniature reaction wheels (RW), magnetorquers and Sun sensors is proposed, similar to that detailed in Kalman.⁷ To maximise available internal volume, Sun sensors and magnetorquers shall be embedded into the Solar panels.

An alternative method of Attitude Control is considered through employment of Control Moment Gyroscopes (CMGs), in place of RWs. CMGs are able to provide a higher torque to mass ratio, and could therefore either reduce mass for equivalent performance, or increase agility for equivalent mass. This has particular benefits should off-nadir pointing be desired to increase potential scientific return. This will not be considered however in this baseline design.

Communication

The communication system provides the necessary capabilities for the transfer of data to and from the ground, be it transfer of commands from the user or transfer of data from the S/C. The amount of usable data obtained by the user, from Charybdis, will depend on the relative position of the platforms (over an area of interest or not), the downlink methodologies employed (direct to particular GS, via many GSs or via Data Relay Satellites) and capabilities of the System (On-board processing, data downlink performance etc).

Due to the high volume of potential data available from each 'Charybdis' platform, an S-band transceiver is considered necessary. Whilst data-rates of $\sim 1\text{-}2\text{Mbit/s}$ are possible from current systems, technological developments indicate data-rates of up to 4Mbit/s can be considered likely in the near-term.²⁰ Furthermore, a conservative lossless compression capability of 2:1 will be assumed present.

For Mission A (altitude = 707.8km), complete image capture of the world's surface would be ideal, however

the sheer volume of data, in addition to the platform limitations, render this impossible. Instead, it is envisaged that organisations would be able to select regions over which images shall be captured. The maximum amount of ground area available can be calculated based on any particular system design and data transfer philosophy.

Assuming utilisation of geostationary data-relay satellites (such as Inmarsat or the proposed EDRS satellites), continuous up/down link availability can be expected, resulting in communications being ‘Charybdis-limited’. Considering ‘useful’ (i.e. daylight) data collection to be possible for 50% of the satellite orbit, this equates to a total potential data capture of ~95.3Gbit (compressed to 47.6Gbit). Considering an orbit period of 5927 seconds, and a data transfer rate of 4Mbit/s, the absolute maximum amount of data transferable to the ground is 23.7Gbit, which equates to ~50% total coverage. This is likely to be closer to ~25% accounting for up-link command requirements and other performance limitations. This equates to ~5.92x10⁵ km² per orbit.

In the case of Mission B (altitude of 573.9km), assuming that communication is made via the Strathclyde University ‘Satellite Tracking and Command Station’ (STAC) only (location of the 55°51.45’N, 004°14.43’W), and a minimum contact elevation angle of 5°, the following general properties can be found (Table 9):

Table 9: STAC Communication parameters

Parameter	Value	Units
Minimum number of contact passes per day	2	-
Maximum number of contact passes per day	4	-
Average contact pass duration	7.9	mins
Minimum contact pass duration per day	15.8	mins
Percentage of total data transferred	69.8	%

It is clear that with the proposed system design and complete coverage of the UK mainland requested, not all of the collected data could be transferred from the satellite (69.8%). Some level of compromise may have to exist therefore, either by further limiting the region of interest, or relaxing the payload performance requirements. For the purpose of this study however, it is shown that a mission of this type could be made feasible in terms of communication links.

Thermal

As with the majority of other CubeSat platforms, it is proposed that ‘Charybdis’ is passively cooled via radiation to deep space and heated via a combination of solar radiation, Earth IR radiation and internal, low-profile heater elements. Temperature sensors can be embedded into the solar panels to enable efficient

MPPT and integrated onto Printed Circuit Boards (PCBs) in order to monitor internal thermal properties.

CONCLUSIONS

It has been shown that a constellation of nanosatellites, named ‘Charybdis’, equipped with multi-spectral imaging payloads, in specific orbits can provide tidal-synchronous, high spatial and temporal resolution radiometry data of ocean colour. Global coverage between latitudes of ±80°, every two hours between 0800 and 1600hrs (local time) can be obtained with a constellation of 115 satellites, while equivalent coverage at specific regions can be achieved with significantly fewer platforms (latitude and longitude boundary dependent). As an example, coverage of the UK mainland can be achieved with as few as 30 platforms, with 50 platforms providing the same regional coverage but with greater potential for growth to global coverage with increase in demand.

A circular tidal synchronous orbit is defined using the following four parameters (prescription of *p* & *q* is not necessary for successful tidal synchronism, but recommended for regional coverage) (Table 10):

Table 10: Orbit parameter variables

Param.	Description
<i>m</i>	No. complete tidal lunar days before exact GT repeat
<i>n</i>	No. satellite orbits before exact GT repeat (at identical tidal conditions)
<i>p</i>	No. complete Earth revolutions (with respect to orbit plane) before exact GT repeat
<i>q</i>	No. satellite orbits before exact GT repeat

A value of *m* equal to 57 has been shown to represent orbit conditions most similar to those of a SS orbit, which is therefore set as the baseline condition for the ‘Charybdis’ constellation.

It has also been shown that on-board propulsion is considered necessary to maintain tidal-synchronous conditions, with modest amounts of propellant required. The propellant mass is given as a function of system specific impulse, for a 3U, 5kg CubeSat at altitudes between 500km and 800km. Post operational de-orbit procedure is presented following propulsion assisted orbit decay, to the critical orbit altitude of 581km (for this particular platform).

Finally, the system-level design of various subsystems is given, with imager payload properties defined as a function of orbit parameters and area coverage capabilities defined as a function of Communication philosophy;

- i. Global coverage satisfied via data links with Data Relay satellites in Geostationary orbits

- whereby ~25% of the total day-lit surface could be captured and transferred each orbit.
- ii. Regional (UK) coverage satisfied via data link with Strathclyde University Ground Station in Glasgow, UK, whereby 70% of the total region of interest could be captured each orbit.

SUMMARY

Ocean colour continues to provide a vast amount of information deemed crucial to our understanding of many processes affecting life on Earth. The ability to monitor ocean colour with greater spatial and temporal resolution will undoubtedly result in significant improvements to this understanding. The constellation approach to ocean colour remote sensing presented here would present a step change transformation in our ability to monitor and understand oceanic and coastal processes.

REFERENCES

1. Sathyendranath, S, "Remote Sensing of Ocean Colour in Coastal, and Other Optically-Complex, Waters", IOCCG Report Number 3, 2000.
2. IOCCG, "Ocean-Colour Sensors", Website http://www.ioccg.org/sensors_ioccg.html.
3. Van Mol, B and K. Ruddick, "The Compact High Resolution Imaging Spectrometer (CHRIS): the Future of Hyperspectral Satellite Sensors. Imagery of Oostende Coastal and Inland Waters", Airborne Imaging Spectroscopy Workshop, Bruges, 2004.
4. Van Mol, B and K. Ruddick, "Total Suspended Matter Maps From CHRIS Imagery of a Small Island Water Body in Oostende (Belgium)", Proc. of 3rd ESA CHRIS/Proba Workshop, 2005.
5. Stuffer, T, H. Kaufman, S. Hofer, K. Forster, R. Graue, D. Kampf, H. Mehl, G. Schreier, A. Mueller, G. Arnold, H. Bach, U. Benz, F. Jung-Rothenhausler and R. Hayden, "The Advanced German Hyperspectral Mission EnMAP", 55th International Astronautical Congress, 2004.
6. Clark, C, S. Greenland, D. Henry and D. McKee, "Medium Resolution Multispectral Earth Observation from a 5kg Nanosatellite", Pestana Conference Centre, 2010.
7. Kalman, A, A. Reif, D. Berkenstock, J. Mann and J. Cutler, "MISCTM – A Novel Approach to Low-Cost Imaging Satellites", 22nd Annual AIAA/USU Conference on Small Satellites, 2008.
8. Fortescue, P, J. Stark and G. Swinerd, "Spacecraft Systems Engineering", 3rd Edition, Wiley-Blackwell, 2003.
9. IOCCG, "Minimum Requirements for an Operational, Ocean-Colour Sensor for the Open Ocean", IOCCG Report Number 1, 1998.
10. Larson, W and J. Wertz, "Space Mission Analysis and Design", 3rd Edition, Space Technology Library, Microcosm, 1999.
11. Mathworks, "Radius at Geocentric Latitude", Website www.mathworks.co.uk/help/toolbox/aeroblae/radiusatgeocentriclatitude.html.
12. Williams, E, "Clairaut's Formula", Aviation Formulary V1.46 Website, williams.best.vwh.net/avform.htm#Clairaut.
13. NOAA, NASA and USAF, "US Standard Atmosphere, 1976", U.S. Government Printing Office, 1976.
14. Macdonald, M, C. Lucking and C. McInnes, "Deployable Gossamer Sail for Deorbiting, Overview of Needs, state of the Art and Deorbiting Mission Scenario", ARTES-5.1 Workplan, 2010.
15. Mueller, J, R. Hofer and J. Ziemer, "Survey of Propulsion Technologies Applicable to CubeSats", Jet Propulsion Laboratory, 2010.
16. Coletti, M, F. Guarducci and S. Gabriel, "A Micro PPT for CubeSat Application: Design and Preliminary Experimental Results", Acta Astronautica, Vol. 69, Issues 3-4, 2011.
17. Sanders, B, L. Van Vliet, F.T. Nardini, T.A. Gronland, P. Rangsten, H. Shea, M. Noca, R. Visee, B. Monna, J. Stark, A. Bulit and A.M. Di Cara, "Development of MEMS based Electric Propulsion", Space Propulsion Conference 2010, San Sebastian, 2010.
18. European Space Agency, "SP-1301: Position Paper on Space Debris Mitigation, Implementing Zero Debris Creation Zones", 2005.
19. Munakata, R, "CubeSat Design Specification", Revision 11, 2008.
20. Greenland, S and C. Clark, "CubeSat Platforms as an On-Orbit Technology Validation and Verification Vehicle", Pestana Conference Centre, Portugal, 2010.